



---

College of Natural and Applied Sciences

---

1-1-2019

## Unravelling the baffling mystery of the ultrahot wind phenomenon in white dwarfs

Nicole Reindl

M. Bainbridge

N. Przybilla

S. Geier

M. Prvák

*See next page for additional authors*

Follow this and additional works at: <https://bearworks.missouristate.edu/articles-cnas>

---

### Recommended Citation

Reindl, Nicole, M. Bainbridge, N. Przybilla, S. Geier, Milan Prvák, Jiří Krtička, R. H. Østensen, J. Telting, and K. Werner. "Unravelling the baffling mystery of the ultrahot wind phenomenon in white dwarfs." *Monthly Notices of the Royal Astronomical Society: Letters* 482, no. 1 (2019): L93-L98.

This article or document was made available through BearWorks, the institutional repository of Missouri State University. The work contained in it may be protected by copyright and require permission of the copyright holder for reuse or redistribution.

For more information, please contact [BearWorks@library.missouristate.edu](mailto:BearWorks@library.missouristate.edu).

---

## Authors

Nicole Reindl, M. Bainbridge, N. Przybilla, S. Geier, M. Prvák, J. Krtička, Roy Østensen, J. Telting, and K. Werner



# Unravelling the baffling mystery of the ultrahot wind phenomenon in white dwarfs

Nicole Reindl,<sup>1</sup>★ M. Bainbridge,<sup>1</sup> N. Przybilla,<sup>2</sup> S. Geier,<sup>3</sup> M. Prvák,<sup>4</sup> J. Krtićka,<sup>4</sup> R. H. Østensen,<sup>5</sup> J. Telting<sup>6</sup> and K. Werner<sup>7</sup>

<sup>1</sup>Department of Physics and Astronomy, University of Leicester, University Road, Leicester LE1 7RH, UK

<sup>2</sup>Institut für Astro- und Teilchenphysik, Universität Innsbruck, Technikerstr. 25/8, A-6020 Innsbruck, Austria

<sup>3</sup>Institute for Physics and Astronomy, University of Potsdam, Karl-Liebknecht-Str. 24/25, D-14476 Potsdam, Germany

<sup>4</sup>Department of Theoretical Physics and Astrophysics, Masaryk University, Kotlářská 2, CZ-611 37 Brno, Czech Republic

<sup>5</sup>Department of Physics, Astronomy and Materials Science, Missouri State University, Springfield, MO 65897, USA

<sup>6</sup>Nordic Optical Telescope, Rambla José Ana Fernández Pérez 7, E-38711 Breña Baja, Spain

<sup>7</sup>Institute for Astronomy and Astrophysics, Kepler Center for Astro and Particle Physics, Eberhard Karls University, Sand 1, D-72076 Tübingen, Germany

Accepted 2018 October 1. Received 2018 September 23; in original form 2018 September 23

## ABSTRACT

The presence of ultrahigh excitation (UHE) absorption lines (e.g. O VIII) in the optical spectra of several of the hottest white dwarfs poses a decades-long mystery and is something that has never been observed in any other astrophysical object. The occurrence of such features requires a dense environment with temperatures near  $10^6$  K, by far exceeding the stellar effective temperature. Here we report the discovery of a new hot wind white dwarf, GALEX J014636.8+323615. Astonishingly, we found for the first time rapid changes of the equivalent widths of the UHE features, which are correlated to the rotational period of the star ( $P = 0.242035$  d). We explain this with the presence of a wind-fed circumstellar magnetosphere in which magnetically confined wind shocks heat up the material to the high temperatures required for the creation of the UHE lines. The photometric and spectroscopic variability of GALEX J014636.8+323615 can then be understood as consequence of the obliquity of the magnetic axis with respect to the rotation axis of the white dwarf. This is the first time a wind-fed circumstellar magnetosphere around an apparently isolated white dwarf has been discovered and finally offers a plausible explanation of the ultrahot wind phenomenon.

**Key words:** stars: AGB and post-AGB – stars: evolution – stars: magnetic field.

## 1 INTRODUCTION

White dwarfs represent the end product of evolution for the vast majority of all stars. Amongst the hottest white dwarfs, i.e. white dwarfs with effective temperatures ( $T_{\text{eff}}$ ) higher than 60 kK, there exists a poorly understood – but nevertheless large – group of objects, which are commonly referred to as hot wind white dwarfs. Different to ordinary hot white dwarfs, the Balmer/He II lines of the hot wind white dwarfs are unusually deep and broad. The majority of the hot wind white dwarfs exhibits broad absorption features in their optical spectra, identified as ultrahigh excitation (UHE) absorption lines (i.e. C V, C VI, N VI, N VII, O VII, O VIII, Ne IX, Ne X). This is something that has never been observed in any other astrophysical object.

The occurrence of these obscure features requires a dense environment with temperatures of the order  $10^6$  K, by far exceeding the

stellar effective temperature. A photospheric origin can therefore be ruled out. Since some of the UHE lines often exhibit an asymmetric profile shape, it was suggested that those lines might form in a hot, optically thick stellar wind (Werner et al. 1995), hence the alternative designation of these stars as hot wind white dwarfs. The physical process responsible for this suspected extremely hot, optically thick stellar wind, however, poses a decades-long mystery.

The fraction of the hottest white dwarfs affected by the ultrahot wind phenomenon is significant. Every other H-deficient white dwarf with  $T_{\text{eff}} > 60$  kK (corresponding to the DO spectral type) belongs to the group of hot wind white dwarfs, and also H-rich white dwarfs are affected by this phenomenon. In total, 18 H-deficient and three H-rich hot wind white dwarfs are currently known (Dreizler et al. 1995; Werner et al. 1995; Werner et al. 2004; Hügelmeier et al. 2006; Reindl et al. 2014; Werner, Rauch & Kepler 2014; Kepler et al. in preparation). In the latter the UHE features are typically weaker and, thus, more difficult to detect. The majority of the hottest H-rich white dwarfs does, however, display the Balmer-line problem (Tremblay, Bergeron & Gianninas 2011), which serves as a first

★ E-mail: nr152@le.ac.uk

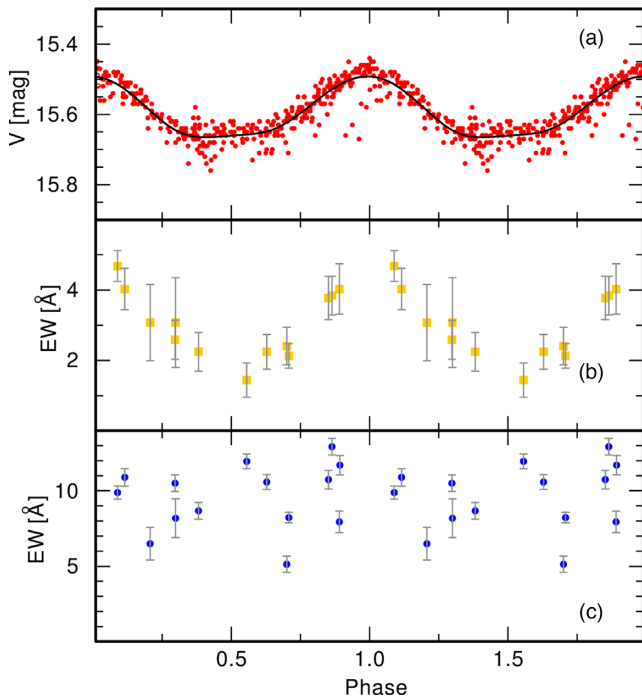


**Figure 1.** Phase folded light curve of J0146+3236 overplotted with a bright-spot model (a). Panels (b) and (c) show the equivalent widths of the UHE feature located at 6060 Å (yellow) and He II  $\lambda$  6560 Å (blue), respectively.

indicator for the hot wind phenomenon. Thus, it may be speculated that a significant fraction of all stars experiences this phenomenon at the beginning of the white dwarf cooling sequence. Therefore, this phenomenon urgently awaits an explanation.

## 2 PHOTOMETRIC OBSERVATIONS

Based on the light curve from the Catalina Sky Survey (CSS) DR1, Drake et al. (2014) classified GALEX J014636.8+323615 (from now on J0146+3236) as a post-common envelope binary with a period of 0.484074 d and a V-band amplitude of 0.17 mag. We obtained the V-band light curve of J0146+3236 released in the CSS DR2. Since the data points are spaced unevenly, we calculated a Lomb-Scargle periodogram (available online) as outlined in Press & Rybicki (1989). We find a period of  $P = 0.242035$  d with a false alarm probability (i.e. the uncertainty associated with the probability that the peak was chosen entirely wrong) of  $2 \times 10^{-51}$ . In Fig. 1 the phase folded light curve is shown. Our derived period is half of that given by Drake et al. (2014), however, they required their folded light curve to have two minima which may have led to an alias in their period estimate. We determine the ephemeris of predicted maxima of the light curve to be  $\text{HJD} = 2456595.98922 + 0.242035(1) E$ .

## 3 SPECTROSCOPIC OBSERVATIONS

We first observed J0146+3236 during a survey exploring candidate sdB stars for the Kepler mission, which were selected from the GALEX survey. The spectrum was taken with the Nordic Optical Telescope using the Alhambra Faint Object Spectrograph and Camera with grism 16 ( $R \approx 1000$ ). Based on this observation, we originally classified J0146+3236 as a normal DO white dwarf. This star was also discovered in the course of the Large Sky Area

Multi-Object Fiber Spectroscopic Telescope (LAMOST; Cui et al. 2012) DR3 by Gentile Fusillo et al. (2015), who also classified J0146+3236 as a DO white dwarf. In 2014 October/November we performed spectroscopic follow-up at the Calar Alto 3.5 m telescope (ProgID H14-3.5-022) using the TWIN spectrograph and a slit width of 1.2 arcsec. We used grating No. T08 for the blue channel and No. T04 for the red channel. The spectra have a resolution of  $1.8 \text{ \AA}$  and a typical signal to noise ratio of 50. A total of 14 spectra of J0146+3236 were taken in three consecutive nights. After each spectrum, we required ThAr wavelength calibration. The data reduction was done using IRAF. We did not flux-calibrate our data. A selection of these spectra along with line identifications is shown in Fig. 2. For comparison, we overplotted a pure He model spectrum with  $T_{\text{eff}} = 100 \text{ kK}$  and  $\log g = 7.5$  that was calculated with the Tübingen non-LTE Model-Atmosphere Package (TMAP; Rauch & Deetjen 2003; Werner et al. 2003; Werner, Dreizler & Rauch 2012). The He II  $\lambda\lambda$  4686, 4859, 5411, 6560 Å lines in the spectra of J0146+3236 appear unusually broad compared to the photospheric DO white dwarf model. The lack of He I  $\lambda$  5876 Å (present in the spectra of some hot wind white dwarfs) indicates an effective temperature in excess of 100 kK. We note, that J0146+3236 is the hitherto brightest known hot wind white dwarf and displays particularly strong UHE absorption lines. These lines have been tentatively identified as Rydberg lines of ultrahigh excited metals. A unique assignment of the lines to particular elements is not possible, although they probably stem from C, N, O, and Ne (Werner, Rauch & Kruk 2018). The TWIN spectra of J0146+3236 also allow for the first time the identification of an additional UHE feature located at 4082 Å. This could be due to C VI  $\lambda$  4084 Å, Al XIII  $\lambda$  4084 Å, O VIII  $\lambda$  4087 Å, or Na XI  $\lambda$  4087 Å (Mohr, Taylor & Newell 2008).

Most astonishingly, however, we discover for the first time rapid changes of the line strengths of several UHE features within about an hour. The TWIN observations were taken one year after the last data point from the CSS allowing us to derive the phase of each spectroscopic observation. We created Voigt profile models of each UHE absorption line using GVPFIT (Bainbridge & Webb 2017) a program based on an ‘Artificial Intelligence’ algorithm, and measured the equivalent widths. Interestingly, we find a clear correlation between the change of the equivalent widths of the UHE lines and the light-curve variability. As can be seen from panel (b) in Fig. 1 the equivalent widths of the UHE lines increase as the object becomes brighter, i.e. reaching the maximum at  $\Phi \approx 0$ , while at  $\Phi \approx 0.5$  some of the lines completely vanish. We also found variations in the equivalent widths of the He II lines, however, these appear randomly as illustrated in panel (c) of Fig. 1 for He II  $\lambda$  6560 Å.

## 4 DISCUSSION

The observed photometric period and the amplitude of the light curve are too high to be attributed to pulsations. Periods and amplitudes of hot, pulsating white dwarfs (i.e. the GW Vir stars) are of the order of minutes and a few mmag, respectively (Fontaine & Brassard 2008). It is also unlikely that the photometric variability is caused by the presence of a close companion for several reasons. First, we cannot detect any radial velocity variations of the He II absorption lines larger than  $14.2 \text{ km s}^{-1}$ . Therefore, a possible companion should have either a high inclination angle or a low mass. The shape of light curve of J0146+3236 resembles that of SDSS J212531.92–010745.8 (Nagel et al. 2006; Schuh, Beeck & Nagel 2009; Shimansky et al. 2015). This system is composed of hot a H-deficient white dwarf and a close, low-mass main-sequence

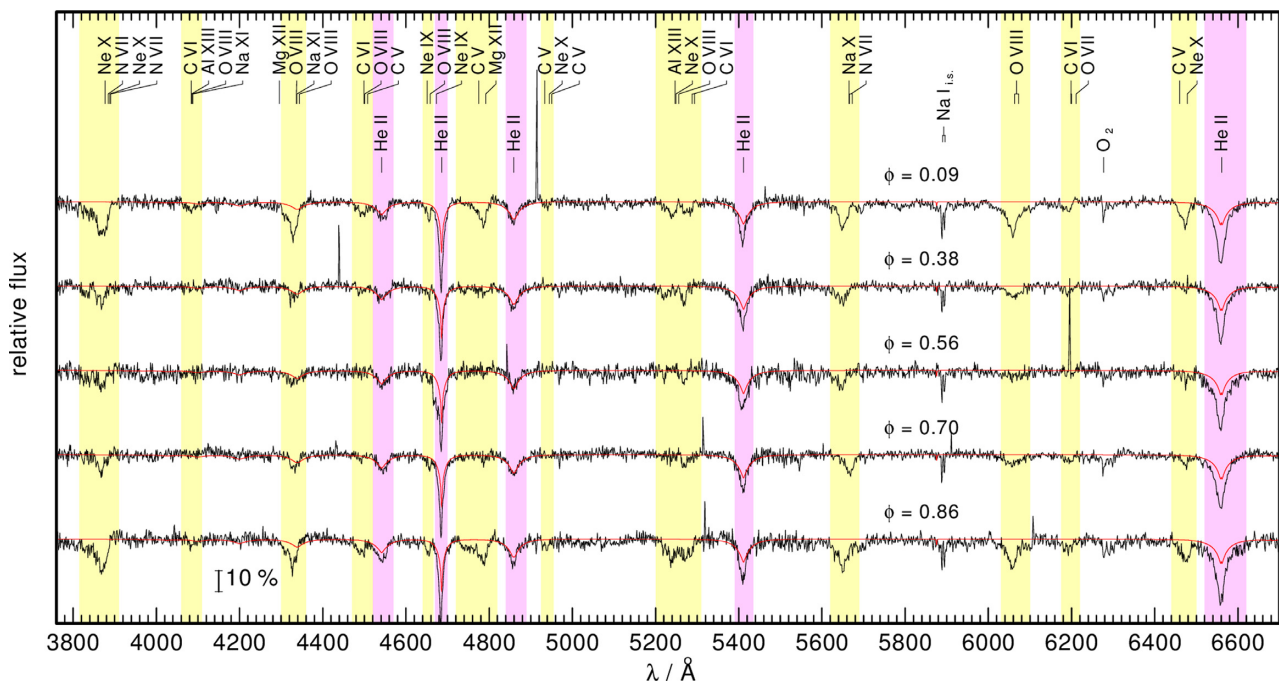


**Figure 2.** TWIN spectra (grey) of J0146+3236. Overplotted is a pure He TMAP model with  $T_{\text{eff}} = 100$  kK and  $\log g = 7.5$  (red). He lines are highlighted in pink and UHE features in yellow. Identified lines are marked. The vertical bar indicates 10 per cent of the continuum flux.

companion ( $P = 0.29$  d). In that case the shape of the light curve is caused by the reflection effect of the cool companion. However, in contrast to SDSS J212531.92–010745.8, in the spectra of J0146+3236 the hydrogen Balmer series does not appear in emission as expected due to the irradiation of the cool companion by the hot white dwarf. Also an infrared excess, which could reveal the presence of a possible companion, cannot be detected.<sup>1</sup>

Interpreting the photometric period as the rotation period of the star, a spot on the surface of the white dwarf could explain the photometric variability. Convection can be ruled out as at such high effective temperatures the atmospheres are radiative. Hence, this spot must be generated by a magnetic field. Spots have been detected on several hot ( $T_{\text{eff}} > 30$  kK), magnetic white dwarfs, causing similar amplitudes in the light curves at the rotation period of the star (Hermes et al. 2017b). Most magnetic white dwarfs are slow rotators (as it occurs for non-magnetic white dwarfs; Fontaine & Brassard 2008), i.e. they show rotation periods of several hours to days (Kawaler 2004; Hermes et al. 2017a). We stress, at such a low rotation rate ( $v_{\text{rot}} = 1$  km s<sup>−1</sup>, assuming a typical white dwarf radius of  $0.02 R_{\odot}$ ), rotational broadening is not detectable in spectra. The sharp cores of the He II lines in the spectra of J0146+3236 (and that of all other hot wind white dwarfs) show no evidence of Zeeman splitting, suggesting an upper limit on the magnetic field strength of 100 kG. Note that spots have been detected on white dwarfs with even lower magnetic field strengths (Hermes et al. 2017a).

The black line in panel (b) of Fig. 1 shows that the shape of the light curve of J0146+3236 could be explained with a bright-spot model assuming an inclination of  $i = 50^{\circ}$ . The synthetic light curve was calculated with a surface brightness distribution that provides the best match to the observed light curve as outlined in Prvák et al. (2015). Our model assumes a brightness of slightly over 125 per cent relative to the rest of the stellar surface and the final surface brightness distribution is available as an online figure. Spots on hot white dwarfs are actually expected to be caused by the accumulation of metals around the magnetic poles (Hermes et al. 2017c), but such models would predict much lower amplitudes for the light curve ( $< 0.1$  mag for hot white dwarfs; Krtićka in preparation). Yet, a magnetic field offers another attractive explanation for the photometric variation and the occurrence of the variable UHE features, namely the presence of a wind-fed circumstellar magnetosphere.

Such magnetospheres develop through the trapping of wind by closed magnetic loops and are commonly observed in magnetic O- and B-type main-sequence stars (Owocki et al. 2016). The accelerated wind material, from opposite footpoints of closed magnetic loops, collides near the loop apex leading to magnetically confined wind shocks (MCWS; Babel & Montmerle 1997; Ud-Doula & Nazé 2016). These MCWSs heat up the magnetically confined plasma (typically located within a few stellar radii of the stellar surface) to several MK (Ud-Doula & Nazé 2016; Wade & Neiner 2018), as required for the creation of the UHE lines observed in the hot wind white dwarfs.

Magnetohydrodynamic (MHD) simulation studies (e.g. Ud-Doula & Owocki 2002; Ud-Doula, Owocki & Townsend 2008) show that the overall net effect of a large-scale, dipole magnetic field can be characterized by the wind magnetic confinement parameter  $\eta_{\star} = \frac{B_{\text{eq}}^2 R_{\star}^2}{\dot{M}_{B=0} v_{\infty}}$ , where  $B_{\text{eq}}$  is the field strength at the magnetic equatorial surface radius  $R_{\star}$ , and  $\dot{M}_{B=0}$  and  $v_{\infty}$  are the fiducial mass-loss rate and terminal wind speed that the star would have in the absence of any magnetic field. For  $\eta_{\star} > 1$ , outflow near

<sup>1</sup>For this, we obtained FUV, NUV (Bianchi, Conti & Shiao 2014),  $u$ ,  $g$ ,  $r$ ,  $i$ ,  $z$  (Ahn et al. 2012),  $J$ ,  $H$  (Cutri et al. 2003), and  $W1$  (Cutri et al. 2012) magnitudes of J0146+3236 and converted them into fluxes as outlined in Reindl et al. (2016). We applied a reddening of  $E_{B-V} = 0.05$  (Schlafly & Finkbeiner 2011) to the flux of our TMAP model mentioned above. Thereafter, we normalized the reddened model flux to the  $g$  magnitude and found that broad-band colour measurements agree within  $3\sigma$  with the model flux.



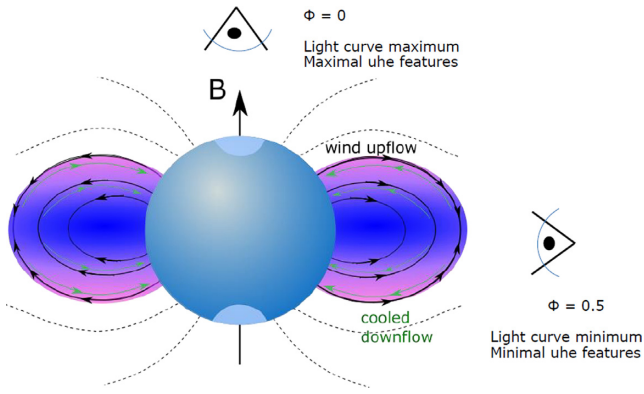


**Figure 3.** Schematic of J0146+3236 (blue) and its circumstellar environment as seen from the perspective of the star’s magnetic axis. Wind material is trapped within closed magnetic loops (black lines) and shock heated. The UHE lines are produced at high latitudes in the magenta region. This shock-heated plasma then cools and falls back on to the star along closed magnetic field lines (green lines). The rotation axis of the white dwarf is inclined by  $45^\circ$  to the magnetic axis and also by  $\approx 45^\circ$  to the observer. At phase 0, we see the system magnetic pole on, the light curve has its maximum because the entire shock-heated torus and possibly a bright-spot are visible. The strengths of the UHE lines is maximal. At phase 0.5 some of the torus is occulted by the star and the strengths of the UHE features becomes minimal.

the magnetic equator is trapped within the Alfvén radius by closed magnetic loops, forming a wind-fed circumstellar magnetosphere. If we assume for J0146+3236 a typical white dwarf radius of  $R_* = 0.02 R_\odot$ , a mass of  $M = 0.6 M_\odot$ , and  $T_{\text{eff}} = 100 \text{ kK}$ , then the mass-loss rate is expected to be  $\dot{M}_{B=0} = 10^{-11} M_\odot \text{ yr}^{-1}$  and the terminal wind velocity about  $10^4 \text{ km s}^{-1}$  (Unglaub & Bues 2000). In that case the requirement for a wind-fed circumstellar magnetosphere is already fulfilled for  $B_{\text{eq}} > 0.6 \text{ kG}$  (well below the upper limit of  $100 \text{ kG}$  drawn from the absence of Zeeman splitting).

The periodic variation of the UHE lines and the light curve can then be understood with the following scenario which we illustrate in Fig. 3. The star is represented in blue, the spots at the magnetic poles in light blue, and the circumstellar magnetosphere in blue, purple, and magenta. The density of the magnetosphere is expected to increase towards lower latitudes, while the temperature is expected to decrease starting with  $\approx 10^6$  to  $10^7 \text{ K}$  at high latitudes (origin of the UHE lines) and reaching the photospheric  $T_{\text{eff}}$  near the magnetic equator (Owocki et al. 2016). Let us assume that the magnetic dipole field is tilted, with respect to the rotation axis, by  $\approx 45^\circ$ . At phase 0 we see the system magnetic pole-on and the maximum amount of the hot post-shock gas located at high latitudes. Therefore, the strengths of the UHE lines is maximal. Also the light curve has its maximum, as the entire shock-heated torus and possibly a bright-spot are visible. As the star rotates the torus becomes partly occulted by the star, the projected area of the torus decreases, and the cooler parts of the magnetosphere come to the fore. Thus, the light curve diminishes, reaching its minimum phase 0.5 when we see the system edge-on. Also the strengths of the UHE features decreases as less of hot post-shock gas from the high latitudes of magnetosphere is visible in the edge-on view.

We note that the variability of the UHE lines in J0146+3236 is similar to what is observed in  $\theta$  Ori C, a O-type main-sequence star hosting a circumstellar magnetosphere and whose magnetic axis is also tilted by  $\approx 45^\circ$  with respect to the rotation axis (see e.g. Gagné et al. 2005). Phase resolved Chandra grating observations of  $\theta$  Ori C show that the line fluxes of H- and He-like ions are approximately

30 per cent higher when the system is seen pole-on than when seen edge-on (Gagné et al. 2005). The observation of UHE absorption lines in the spectra of J0146+3236 suggests that the shock-heated plasma must be optically thick, in contrast to the optically thin shock-heated plasma observed in  $\theta$  Ori C, which shows the X-ray UHE lines in emission. X-ray UHE absorption lines have been detected in warm absorbers which are observed in about 50 per cent of the Seyfert galaxies (e.g. Blustin et al. 2002). The column densities of these warm absorbers which surround the active nucleus of these galaxies are of the order of  $10^{22} \text{ cm}^{-2}$  (Komossa 2000). The magnetospheric column density of the shock-heated plasma of  $\theta$  Ori C is slightly lower, namely  $5 \times 10^{21} \text{ cm}^{-2}$  (Gagné et al. 2005). The characteristic wind density,  $\rho_w \equiv \dot{M}_{B=0}/4\pi v_\infty R_*^2 \approx 3 \times 10^{-13} \text{ g cm}^{-3}$ , of J0146+3236 is similar to of  $\theta$  Ori C. We speculate the higher magnetospheric density of J0146+3236 might be related to the fact that low luminosity stars with weak winds experience weaker shocks (Ud-Doula et al. 2014). The slower scaled shock speed,  $\omega_s$ , leads to a cooler post-shock temperature  $T_s \sim \omega_s^2$  (Owocki et al. 2016) and the shock-heated plasma becomes more spatially extended. The subsonic nature of the post-shock flow implies a nearly constant pressure ( $P \sim \rho T$ ), meaning that the density increases strongly as temperature declines (see fig. 3 in Owocki et al. 2016). Hence, we would expect for the hot wind white dwarfs a higher density and lower temperature magnetosphere (of the order  $10^6 \text{ K}$  instead of  $10^7 \text{ K}$ ) than what is observed for O- and B-type main-sequence stars that host circumstellar magnetospheres.

The cooler parts of the magnetosphere then likely constitute an additional line forming region of the too-broad and too-deep He II lines. Werner et al. (2018) already speculated these lines could be caused by relatively cool gas in a circumstellar static cloud. Similarly, variable optical helium lines, like He II  $\lambda 4684 \text{ \AA}$ , in magnetic O-stars show clear signatures of being formed in a dynamical magnetosphere (Grunhut et al. 2012; Wade et al. 2015). Ud-Doula & Owocki (2002) showed that the shock-heated wind plasma eventually cools radiatively back to temperatures near the stellar effective temperature and then falls back on to the stellar surface along closed magnetic field lines on a dynamical (free-fall) time-scale. The infall of the cooled material occurs in sporadic intervals of highly compressed, localized streams (Owocki et al. 2016), which may explain the random variations of the equivalent widths of the He II lines.

Having in mind that the UHE features diminish when we see the system edge-on, this scenario also naturally explains why some objects only show abnormal broad and deep optical H and He II lines, but no UHE lines. Another possibility is that these stars have an even slower scaled shock speed and, thus, a cooler post-shock plasma. A similar argument may hold for H-rich white dwarfs, amongst which the ultra-hot wind phenomenon seems less common. H-rich objects have lower  $v_\infty$  compared to their H-deficient counterparts (Pauldrach et al. 1988), therefore a lower post-shock temperature ( $T_s \sim v_\infty^2$ ) would be expected. We also note that the variability of the UHE lines is only expected if the magnetic and rotation axis are tilted.

## 5 SUMMARY AND CONCLUSIONS

We report about the discovery of a new hot wind white dwarf, J0146+3236, that reveals rapid changes of the equivalent widths of several UHE features, which are correlated to the star’s rotation period ( $P = 0.242035 \text{ d}$ ). We present a physical model that, finally, offers a plausible explanation of the ultra-hot wind phenomenon. A weak magnetic field ( $\approx 0.6\text{--}100 \text{ kG}$ ) channels the wind material toward the magnetic equator, forming a dense, wind-fed circumstellar

magnetosphere. MCWSs heat up the material to the high temperatures required for the creation of the UHE lines. As the star's magnetic axis (i.e. the axis of the torus) is tilted with respect to the rotation axis, the brightness and intensity of the UHE features vary as a function of the rotation phase of the star. The radiatively cooled and dense post-shock material in the magnetosphere sporadically falls back on to the stellar surface and constitutes an additional line forming region for the variable, too-broad and too-deep He II lines. This is the first time that a wind-fed circumstellar magnetosphere around an apparently isolated white dwarf has been discovered. About 25 per cent of all white dwarfs have weak magnetic field strengths of a few kG (Aznar Cuadrado et al. 2004), suggesting that indeed a substantial fraction of all stars may develop a wind-fed circumstellar magnetosphere during their early white dwarf cooling phase. We like to emphasize that this discovery may have far-reaching consequences. The neglect of the magnetospheric contribution to the optical H and He II lines could lead to large systematic effects on the derived effective temperatures and surface gravities of these stars, and consequently on all other properties obtained from those (e.g. the mass distributions and luminosity functions of hot white dwarfs). In addition wind magnetic spin-down (Ud-Doula, Owocki & Townsend 2009) could have a noticeable impact on the angular momentum evolution of these stars.

Further theoretical and observational effort is therefore highly desirable for a profound understanding of the hot wind white dwarfs. Spectro-polarimetric observations may help to derive the magnetic field strengths of the hot wind white dwarfs. MHD simulations and a detailed line profile analysis of the UHE features would allow us to investigate the physics of the shock heated plasma. Time-resolved, high S/N UV spectra (that is where photospheric metals can be detected) could reveal chemical spots and possible signatures of a weak, phase dependent wind in the UV resonance lines. Detailed light curve modelling could help to understand the origin of the photometric variability more and reveal the geometry of these extraordinary systems.

## ACKNOWLEDGEMENTS

Based on observations collected at the German-Spanish Astronomical Center, Calar Alto, jointly operated by the Max-Planck-Institut für Astronomie Heidelberg and the Instituto de Astrofísica de Andalucía (CSIC). We thank JJ Hermes for helpful discussions and comments. NR is supported by a Royal Commission 1851 research fellowship. MB is supported by a Leverhulme Trust Research Project Grant. SG acknowledges funding by the Heisenberg program of the Deutsche Forschungsgemeinschaft under grant GE 2506/8-1. MP and JK were supported by grant GA ČR 16-01116S. This research used the ALICE High Performance Computing Facility at the University of Leicester. The CSS survey is funded by the National Aeronautics and Space Administration under Grant No. NNG05GF22G issued through the Science Mission Directorate Near-Earth Objects Observations Program. The CRTS survey is supported by the U.S. National Science Foundation under grants AST-0909182.

## REFERENCES

Ahn C. P. et al., 2012, *ApJS*, 203, 21  
 Aznar Cuadrado R., Jordan S., Napiwotzki R., Schmid H. M., Solanki S. K., Mathys G., 2004, *A&A*, 423, 1081  
 Babel J., Montmerle T., 1997, *A&A*, 323, 121  
 Bainbridge M. B., Webb J. K., 2017, *MNRAS*, 468, 1639

Bianchi L. et al., 2011, *MNRAS*, 411, 2770  
 Blustin A. J., Branduardi-Raymont G., Behar E., Kaastra J. S., Kahn S. M., Page M. J., Sako M., Steenbrugge K. C., 2002, *A&A*, 392, 453  
 Cui X.-Q. et al., 2012, *Res. Astron. Astrophys.*, 12, 1197  
 Cutri R. M. et al., 2003, VizieR Online Data Catalog, 2246, 0  
 Cutri R. M. et al., 2012, Explanatory Supplement to the WISE All.Sky Data Release Products, 1  
 Drake A. J. et al., 2014, *ApJS*, 213, 9  
 Dreizler S., Heber U., Napiwotzki R., Hagen H. J., 1995, *A&A*, 303, L53  
 Fontaine G., Brassard P., 2008, *PASP*, 120, 1043  
 Gagné M., Oksala M. E., Cohen D. H., Tonnesen S. K., ud-Doula A., Owocki S. P., Townsend R. H. D., MacFarlane J. J., 2005, *ApJ*, 628, 986  
 Gentile Fusillo N. P. et al., 2015, *MNRAS*, 452, 765  
 Grunhut J. H. et al., 2012, *MNRAS*, 426, 2208  
 Hermes J. J. et al., 2017a, *ApJS*, 232, 23  
 Hermes J. J., Gänsicke B. T., Gentile Fusillo N. P., Raddi R., Hollands M. A., Denny E., Fuchs J. T., Redfield S., 2017b, *MNRAS*, 468, 1946  
 Hermes J. J., Kawaler S. D., Bischoff-Kim A., Provencal J. L., Dunlap B. H., Clemens J. C., 2017c, *ApJ*, 835, 277  
 Hügelmeier S. D., Dreizler S., Homeier D., Krzesiński J., Werner K., Nitta A., Kleinman S. J., 2006, *A&A*, 454, 617  
 Kawaler S. D., 2004, in Maeder A., Eneen P., eds, *Proc. IAU Symp. Vol. 215, Stellar Rotation*. Kluwer, Dordrecht, p. 561  
 Komossa S., 2000preprint (arXiv:astr-ph/0001263)  
 Mohr P. J., Taylor B. N., Newell D. B., 2008, *Rev. Mod. Phys.*, 80, 633  
 Nagel T., Schuh S., Kusterer D.-J., Stahn T., Hügelmeier S. D., Dreizler S., Gänsicke B. T., Schreiber M. R., 2006, *A&A*, 448, L25  
 Owocki S. P., ud-Doula A., Sundqvist J. O., Petit V., Cohen D. H., Townsend R. H. D., 2016, *MNRAS*, 462, 3830  
 Pauldrach A., Puls J., Kudritzki R. P., Méndez R. H., Heap S. R., 1988, *A&A*, 207, 123  
 Press W. H., Rybicki G. B., 1989, *ApJ*, 338, 277  
 Prvák M., Liška J., Krtička J., Mikulášek Z., Lüftinger T., 2015, *A&A*, 584, A17  
 Rauch T., Deetjen J. L., 2003, in Hubeny I., Mihalas D., Werner K., eds, *ASP Conf. Ser. Vol. 288, Handling of Atomic Data*. Astron. Soc. Pac., San Francisco, p. 103  
 Reindl N., Rauch T., Werner K., Kepler S. O., Gänsicke B. T., Gentile Fusillo N. P., 2014, *A&A*, 572, A117  
 Reindl N., Geier S., Kupfer T., Bloemen S., Schaffenroth V., Heber U., Barlow B. N., Østensen R. H., 2016, *A&A*, 587, A101  
 Schlafly E. F., Finkbeiner D. P., 2011, *ApJ*, 737, 103  
 Schuh S., Beeck B., Nagel T., 2009, *J. Phys. Conf. Ser.*, 172, 012065  
 Shimansky V. V., Borisov N. V., Nurtidina D. N., Solovyeva Y. N., Sakhibullin N. A., Spiridonova O. I., 2015, *Astron. Rep.*, 59, 199  
 Tremblay P.-E., Bergeron P., Gianninas A., 2011, *ApJ*, 730, 128  
 Ud-Doula A., Nazé Y., 2016, *Adv. Space Res.*, 58, 680  
 Ud-Doula A., Owocki S. P., 2002, *ApJ*, 576, 413  
 Ud-Doula A., Owocki S. P., Townsend R. H. D., 2008, *MNRAS*, 385, 97  
 Ud-Doula A., Owocki S. P., Townsend R. H. D., 2009, *MNRAS*, 392, 1022  
 Ud-Doula A., Owocki S., Townsend R., Petit V., Cohen D., 2014, *MNRAS*, 441, 3600  
 Unglaub K., Bues I., 2000, *A&A*, 359, 1042  
 Wade G. A., Neiner C., 2018, *Contrib. Astron. Obs. Skalnaté Pleso*, 48, 106  
 Wade G. A. et al., 2015, *MNRAS*, 447, 2551  
 Werner K., Dreizler S., Heber U., Rauch T., Wisotzki L., Hagen H.-J., 1995, *A&A*, 293, L75  
 Werner K., Deetjen J. L., Dreizler S., Nagel T., Rauch T., Schuh S. L., 2003, in Hubeny I., Mihalas D., Werner K., eds, *ASP Conf. Ser. Vol. 288, Model Photospheres with Accelerated Lambda Iteration*. Astron. Soc. Pac., San Francisco, p. 31  
 Werner K., Rauch T., Napiwotzki R., Christlieb N., Reimers D., Karl C. A., 2004, *A&A*, 424, 657  
 Werner K., Dreizler S., Rauch T., 2012, *Astrophysics Source Code Library record ascl:1212.015*  
 Werner K., Rauch T., Kepler S. O., 2014, *A&A*, 564, A53  
 Werner K., Rauch T., Kruk J. W., 2018, *A&A*, 609, A107

## SUPPORTING INFORMATION

Supplementary data are available at [MNRASL](#) online.

**Lomb\_J0146.png  
map.png**

Please note: Oxford University Press is not responsible for the content or functionality of any supporting materials supplied by

the authors. Any queries (other than missing material) should be directed to the corresponding author for the article.

This paper has been typeset from a  $\text{\TeX/L\AA\TeX}$  file prepared by the author.